Ferrimagnetic resonance in films of vanadium [tetracyanoethanide]$_x$, grown by chemical vapor deposition

R. Plachy,[1] K. I. Pokhodnya,[2,3] P. C. Taylor,[1] J. Shi,[1] Joel S. Miller,[3] and A. J. Epstein[2,4]
[1]*Department of Physics, University of Utah, 115 South 1400 East, Room 201, Salt Lake City, Utah 84112-0830, USA*
[2]*Department of Physics, The Ohio State University, 174 West Eighteenth Avenue, Columbus, Ohio 43210-1106, USA*
[3]*Department of Chemistry, University of Utah, 315 South 1400 East, Room 2020, Salt Lake City, Utah 84112-0850, USA*
[4]*Department of Chemistry, The Ohio State University, 100 West Eighteenth Avenue, Columbus, Ohio 43210-1173, USA*
(Received 16 January 2004; published 18 August 2004)

Ferrimagnetic resonance (FMR) measurements in thin films of V[TCNE]$_x$ grown by chemical vapor deposition exhibit a series of sharp lines at 300 K. The orientational dependence of these lines is a result of the sample geometry provided the magnetization tracks the applied magnetic field. The FMR intensities scale with the temperature dependence of the magnetization as measured by SQUID magnetometry. The temperature dependence of the FMR at various orientations yields an estimate of the local, negative anisotropy field, which is approximately 200 Oe at zero temperature and decreases linearly with increasing temperature and is well fit by a model developed for spin glasses. The widths of the FMR lines track the temperature dependence of the magnetization, which suggests that they are determined by density fluctuations. The spacings between the individual FMR lines and their temperature dependence are consistent with the presence of nonlinear spin waves, whose critical microwave field is approximately 10^{-2} Oe. A rough estimate of the exchange stiffness constant is $A=10^{-10}$ erg/cm. The small value of A may be due to the magnitude of the antiferromagnetic exchange between V and adjacent TCNE and the frustration of AFM exchange between adjacent TCNE radicals.

DOI: 10.1103/PhysRevB.70.064411 PACS number(s): 75.50.Xx, 76.50.+g, 75.30.−m, 75.70.−i

I. INTRODUCTION

Magnets based on organic molecules have been studied for many years.[1] During this time many advances have occurred including the production of materials with magnetic ordering temperatures, T_c, above room temperature[2,3] and the discovery of new types of magnetic phenomena in organic-based magnets.[4] One such system is V[TCNE]$_x$ (where x is approximately 2), in which V^{II} ions coordinate tetracyanoethylene ion-radicals $[TCNE]^-$ to form a three-dimensional network. The original synthesis of V[TCNE]$_x$ involved the use of various solvents.[2–4] The degree of structural order is dependent upon the coordinating ability of the solvent.[5] The random magnetic anisotropy increased with increasing structural disorder.[5] For V[TCNE]$_x$ prepared in noncoordinating CH_2Cl_2, $T_c \sim 400$ K.[2,3,5] For samples prepared in C_4H_9O,[6] the T_c value was reduced to approximately 200 K. The value was further reduced to $T_c \sim 100$ K for samples prepared in CH_3CN.[7,8] The glassy magnetic behavior was more prominent as T_c decreased. A change in the source of V from $V(C_6H_6)_2$ to $V(CO)_6$ in solution prepared samples increased the structural order resulting in less prominent glassy behavior.[9]

Recently the material has been deposited on substrates using a chemical vapor deposition (CVD) process that does not require a solvent.[10,11] In both the CVD-prepared films and the CH_2Cl_2 solution prepared powder samples,[2,3] T_c is approximately 400 K, but the structural disorder is less in the CVD-prepared films.[10] V[TCNE]$_x$ is a ferromagnet with the V^{2+} forming one sublattice and the $[TCNE]^-$ ligands forming the other sublattice. Since the respective spins of these two sublattices are 3/2 and 1 (1/2 for each TCNE), the net spin is 1/2 per formula unit.[2] Earlier ferrimagnetic resonance (FMR) studies of powder samples prepared in CH_3CN solution demonstrated the feasibility of probing the disordered magnetic states with FMR,[13] and the results were analyzed using the Becker model[14] for FMR of spin glasses.

In this paper we report the first FMR studies of thin CVD films of V[TCNE]$_x$, where T_c is above 300 K. Although the details of the FMR spectra in these CVD films depend on the individual sample, the general features, such as the angular dependence of the spectra, the temperature dependence of the linewidths, and the anisotropy factors, are universal properties of all films. These thin films have several advantages in studying the microscopic magnetic properties. First, the FMR exhibits very narrow linewidths near T_c so that both the microscopic, magnetic anisotropies and the anisotropies due to the shape of the film can be studied in detail. Second, the temperature dependence of the FMR as a function of the orientation of the film in the external magnetic field provides an accurate measure of temperature dependences of the anisotropy field and the effective g-values. Third, measurements of the FMR intensities and line widths as functions of temperature provide estimates of the temperature dependence of the saturation magnetization and the porosity of the films, respectively. Finally, the occurrence of spin waves in the nonlinear regime provides an estimate of the exchange stiffness constant.

Inhomogeneities play a role in two of the FMR properties of the CVD films of V[TCNE]$_x$. In particular, the linewidth is determined by density fluctuations, and the details

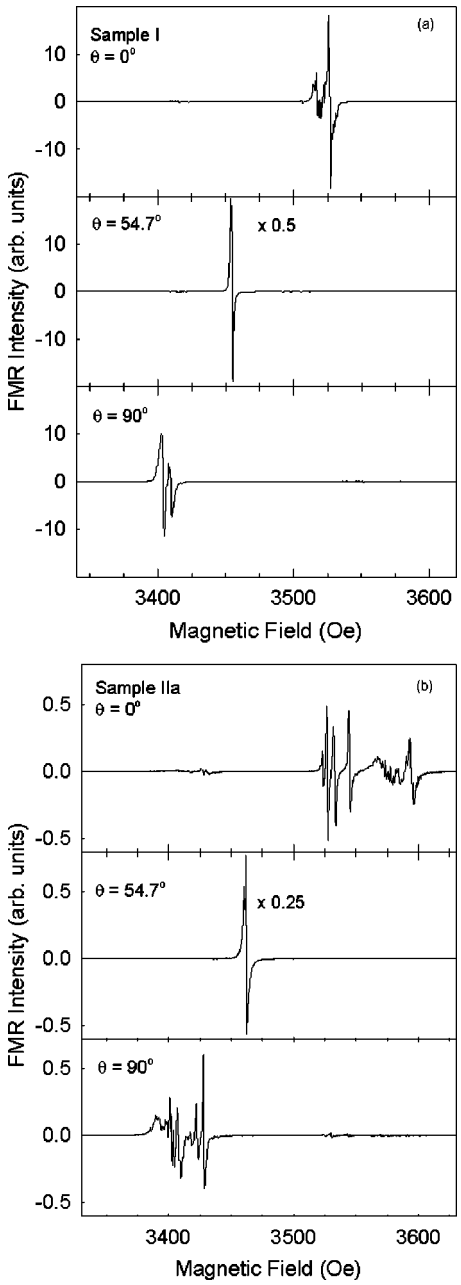

FIG. 1. FMR line shapes of $V[TCNE]_x$ [samples I and IIa in (a) and (b), respectively] at 300 K for the magnetic field parallel ($\theta = 0°$), perpendicular ($\theta = 90°$), and $\theta = 54.7°$ with respect to the normal to the plane of the film. See text for details.

of the nonlinear spin waves also depend on inhomogeneities in the films.

II. EXPERIMENTAL DETAILS

The films of $V[TCNE]_x$ were prepared by chemical vapor deposition (CVD). Bulk samples of $V[TCNE]_x \cdot y(CH_2Cl_2)$ were prepared according to procedures described in the literature.[3] The CH_2Cl_2 used for the reaction was distilled from the appropriate drying agents. Three $V[TCNE]_x$ films were deposited on thin glass substrates ($5 \times 2 \times 0.1$ mm) using the CVD method described in Ref. 10. All manipulations and reactions were performed in an Ar-filled, Vacuum Atmosphere DriLab glove box (~ 1 ppm O_2 and < 1 ppm H_2O) as described in detail elsewhere.[10] Samples for the FMR measurements were sealed in ESR-grade quartz tubes[15] for spectroscopic investigations at approximately 9 GHz. Details of the ESR spectrometer (Bruker, Model EMX) and Helitran variable temperature system used for these studies are available elsewhere.[15]

Three CVD-prepared film samples and one CVD prepared "powder" sample were used for this study. The three film samples, denoted by I, IIa, and IIb, were deposited at a substrate temperature of $40 \pm 1\,°C$, and the thicknesses ranged from about 0.5 to about 2 μm. Samples IIa and IIb were made from a single deposition, and sample I was made from a different deposition using the same substrate temperature and mass-flow parameters. In order to maximize the sample mass, the powder sample was made from material scraped from the walls of the reactor as described in Ref. 10. This powder sample may be less homogeneous than the film samples and may have a different value (or varying values) of x (different composition).

III. EXPERIMENTAL RESULTS

In contrast to the isotropic and generally featureless structures observed in solvent-prepared samples of $V[TCNE]_x$,[3,13] the FMR spectra of the CVD films exhibit a rich structure below the transition temperature (T_c). In addition, at all temperatures the FMR spectra in the films exhibit variations in the resonant frequencies depending on the orientation of the magnetic field with respect to the plane of the film. An example of the data obtained at 300 K is shown in Fig. 1 for samples I and IIa. This figure shows the room temperature FMR measurements (derivative of the FMR absorption spectrum) at approximately 300 K on two thin films of $V[TCNE]_x$ made in different deposition runs with H parallel, perpendicular, and 54.7° from the normal to the plane of the film. (The angle from the normal to the plane will henceforth be designated by θ.) The angular dependence is primarily due to the disklike shape of the sample that produces the standard surface effects, which we shall henceforth characterize using the magnetization vector $\boldsymbol{M}$. One can see clearly from Fig. 1 that the individual linewidths are very narrow at 300 K (approximately 1 Oe peak-to-peak in the derivative spectrum).

The features of the orientational dependence for the 300 K FMR shown in Fig. 1 (and also in Figs. 3 and 7 at 300 K) are easily explained by the standard dependence of the effective magnetization on the shape of the sample. In general, for an infinitely thin disk where the magnetization does not necessarily lie along the applied field $\boldsymbol{H}$, the resonant frequency is given by two equations that must be solved self consistently.[16–18] In our case, where $4\pi\boldsymbol{M} \ll \boldsymbol{H}$ ($\boldsymbol{H}$ is the applied field) at all temperatures, the magnetization does indeed lie along the applied field for all orientations, and the behavior is governed by a single equation,[17,18]

$$H = \left(2\pi M - \frac{H_A}{2}\right)\left\{2 - 3\,\sin^2(\theta) + \left[9\,\sin^4(\theta) - 8\,\sin^2(\theta) + \frac{4H_r^2}{(4\pi M - H_A)^2}\right]^{1/2}\right\}, \quad (1)$$

where H is the applied magnetic field, M is the saturation magnetization, H_A is the random uniaxial anisotropy field, which we shall assume is independent of angle, θ is the angle from the normal to the plane of the film, and H_r is the internal resonant field (i.e., the field at which resonance will occur in the absence of any shape effects). The internal resonant field can be described by an effective g-value, $g_{\text{eff}} = h\nu_0/\mu_B H_r$, where h is Planck's constant, ν_0 is the spectrometer operating frequency, and μ_B is the Bohr magneton.

For the two symmetry directions, $\theta = 0°$ and 90°, Eq. (1) reduces to

$$H(0) = H_\perp = 4\pi M - H_A + H_r, \quad (2)$$

and

$$H(90°) = H_\parallel = \frac{H_A}{2} - 2\pi M + \frac{1}{2}[(4\pi M - H_A)^2 + 4H_r^2]^{1/2}, \quad (3)$$

or

$$H_\parallel \simeq -2\pi M + \frac{H_A}{2} + H_r, \quad (4)$$

where Eq. (4) holds when $4\pi M - H_A \ll H_r$.

The angular dependences of several specific features of the spectra in Fig. 1 are shown in Fig. 2. These features correspond roughly to the lowest, highest and intermediate features in the spectra of Fig. 1 as shown in the inset to Fig. 2. (The bottom trace in the inset to Fig. 2 for $\theta = 90°$ has been inverted about the magnetic field for $\theta = 54.7°$.)

From Eqs. (2) and (4) one can see that there is a specific symmetry of the quantity $4\pi M - H_A$ about H_r. In addition, from Eq. (1) one can show that $H \simeq H_r$ at 54.7°. Therefore, if one reflects the spectrum for $\theta = 90°$ about the position of the narrow resonance, which occurs at $\theta = 54.7°$, and expands the scale by a factor of 2, then the comparison with the spectrum for $\theta = 0°$ is as shown in the inset to Fig. 2. (The vertical axis of the spectrum for $\theta = 90°$ has also been inverted because of the phase introduced by taking the derivative.) One can see from the inset to Fig. 2 that nearly every feature in the spectrum for $\theta = 0°$ is approximately reproduced in the one for $\theta = 90°$, albeit with less resolution. The decrease in resolution for the case where $\theta = 90°$ occurs because the natural linewidth of each individual feature is independent of orientation, and one effectively decreases the resolution when the lines are closer together.

This correspondence clearly indicates that the many "resonances" seen in the spectra are coupled in pairs. They either correspond to different regions in the sample with different values of $4\pi M - H_A$ or to the presence of magnetic excitations with finite wave vector (spin waves). Details will be discussed below.

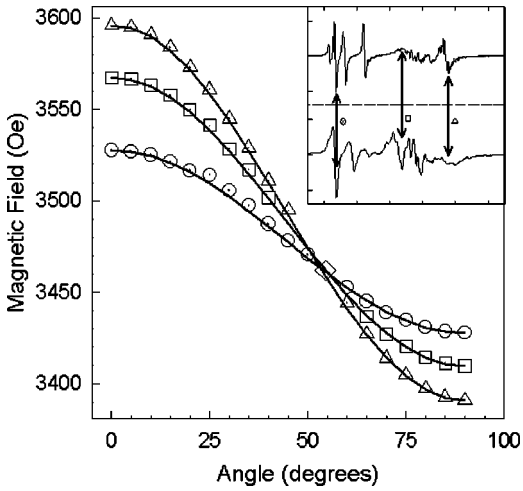

FIG. 2. Angular dependence of three features in the FMR spectra of $V[TCNE]_x$ (sample IIa) at 300 K. The specific features are indicated in the inset. The solid lines are fits to the data as described in the text. The inset shows a comparison of the low field ($\theta = 90°$) and high field ($\theta = 0°$) resonances in $V[TCNE]_x$ (sample IIa). The resonance for $\theta = 0°$ has been reflected about a point 1/3 of the distance to the resonance for $\theta = 0°$ (i.e., about the position of the narrow resonance at 54.7°). The phase has also been inverted (180°) because the spectrum is the derivative of the absorption. The circle, square, and triangle refer to the data as plotted in this figure. See text for details.

The spectra of Fig. 1 exhibit the symmetry predicted by Eq. (1). As shown in the inset to Fig. 2, the position of the resonance at an angle of approximately 54.7° with respect to the plane of the film is twice as far away from the resonance with H perpendicular to the plane of the film ($\theta = 0°$) as it is to the resonance with H parallel to the plane of the film ($\theta = 90°$). In addition, the angle at which the spectra collapse to a single narrow line depends critically on the orientation of $\boldsymbol{M}$ with respect to $\boldsymbol{H}$, and this angle is only 54.7° (corresponding to $3\cos^2(\theta) = 1$) for $\boldsymbol{M}$ always parallel to $\boldsymbol{H}$ [i.e., when Eq. (1) holds] and when $4\pi M \ll H$. The crossover at $\theta = 54.7°$ is only approximate for finite values of $4\pi M - H_A$, and it corresponds to neglecting the square root factor in Eq. (1). Since we shall show that $H_A \simeq 0$ at 300 K, we neglect H_A, and to first order the dependence of the crossing on M can be expressed as

$$H \simeq H_r\left[1 - \frac{2}{3}\left(\frac{2\pi M}{H_r}\right)^2 + \cdots\right]. \quad (5)$$

For the present case $2\pi M$ is approximately 50 G, and the second term in Eq. (5) is less than approximately 0.5 Oe, which cannot be resolved on the scale of Fig. 2.

From an average point on the spectra with $\theta = 0°$ or $\theta = 90°$, one can estimate from Eq. (1) that the magnetization at 300 K is on the order 10 G, if H_A can be ignored, a situation that we shall justify below. Therefore, our approximation that $4\pi M \ll H$ is justified *a posteriori*.

The solid lines through the data in Fig. 2 are fits using Eq. (1) with M scaled to a specific peak at $\theta = 0°$. The three lines correspond to the features shown by the arrows in the inset to

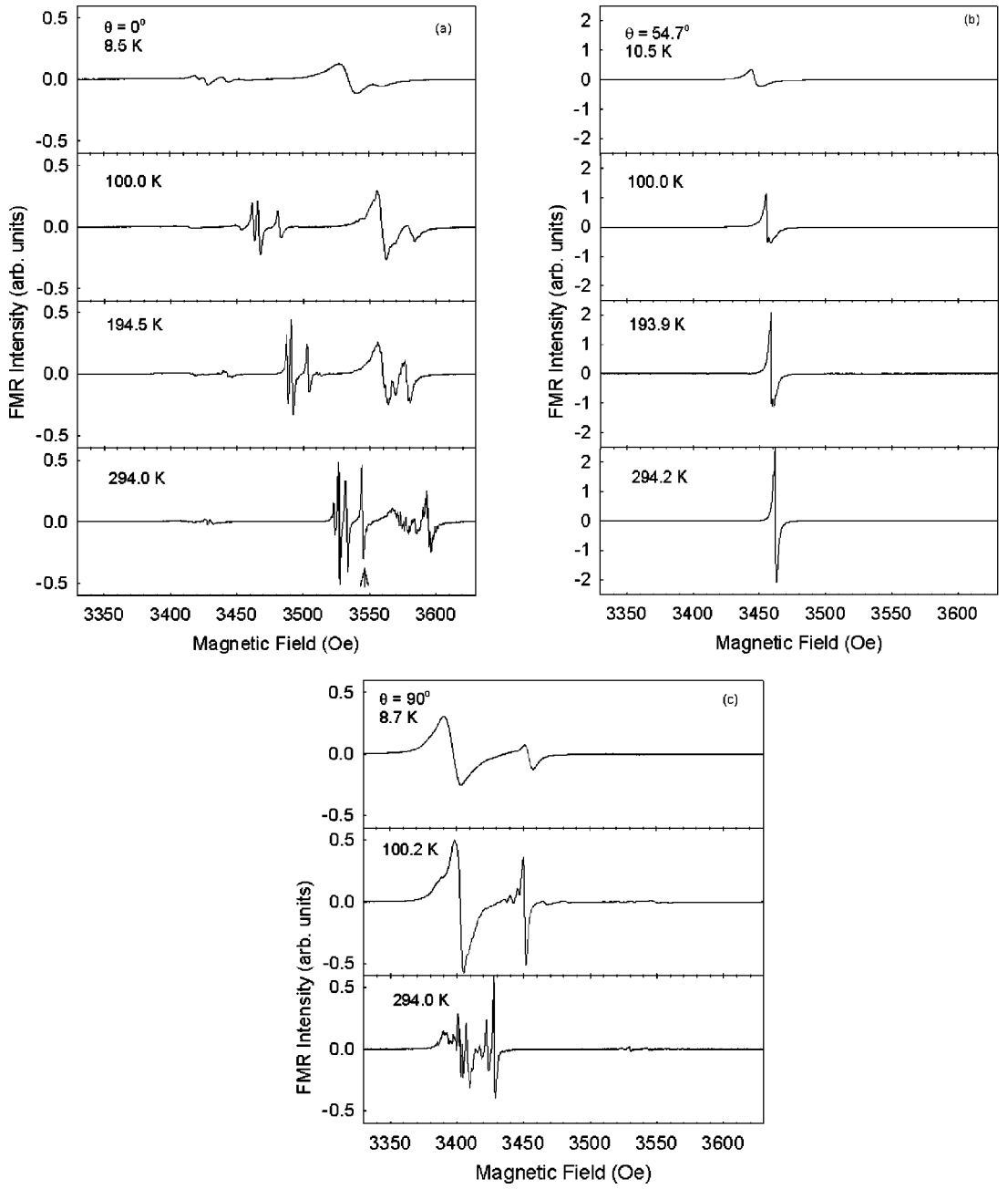

FIG. 3. FMR line shapes in $V[TCNE]_x$ (sample IIa) for (a) $\theta=0°$, (b) $\theta=54.7°$, and (c) $\theta=90°$ at selected temperatures.

Fig. 2. The agreement with the predictions of Eq. (1) is excellent.

As the temperature decreases, especially below about 100 K, the linewidths of the individual features shown in Fig. 1 increase. Figure 3 shows the temperature dependence of the spectra for three values $\theta=0°$, 54.7°, and 90°. In Fig. 4 we show the temperature dependence of the linewidth (peak-to-peak width of the derivative) for an individual line for sample IIa (as indicated by the arrow in Fig. 3). The filled circles are data for a powder CVD-grown sample of $V[TCNE]_x$, which contains no solvent. Note that the linewidths of the powder sample at all temperatures are much greater than those of the film, presumably due to greater inhomogeneities in the powder. The dashed and solid lines are theoretical fits to the data to be discussed in the next section.

The integrated FMR intensity (double integral of the derivative traces) increases as the temperature decreases. This behavior, which is consistent with the temperature dependence of the magnetization, is shown in Fig. 5 for sample IIa for the field perpendicular to the plane of the film ($\theta=0°$). Similar data were obtained for other orientations and other samples (sample I and sample IIb). The specific angle ($\theta=0°$) was chosen because the error in the double integration was smaller. The solid line is a theoretical fit to be discussed below. Figure 6 shows the dependence of the integrated FMR intensity on the applied microwave power for sample IIa at 300 K. Similar data are obtained for all samples at all mea-

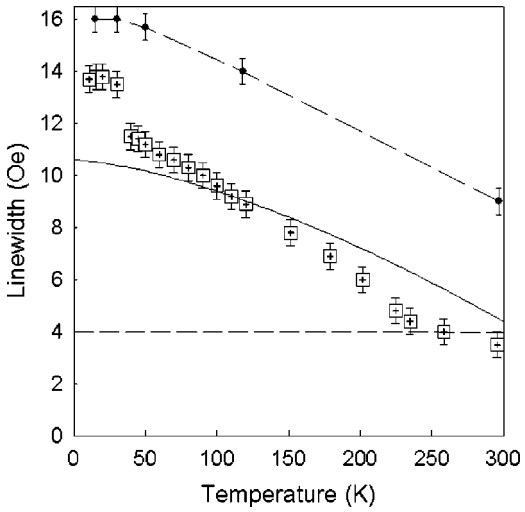

FIG. 4. FMR linewidth (peak-to-peak width of the derivative spectrum) as a function of temperature for $V[TCNE]_x$ (sample IIa, open squares, at $\theta=54.7°$). The dashed and solid lines are model fits to the data assuming the broadening mechanisms are local anisotropy and porosity (or surface roughness), respectively. The filled circles are data for a powder sample, and the long dashed line is an aid to the eye. See text for details.

sured temperatures. The solid line in Fig. 6 is drawn such that the intensity is proportional to the applied microwave magnetic field (square root of the microwave power). One can see from Fig. 6 that the data accurately fit this dependence over the entire range of experimentally accessible microwave fields, and therefore that the double integrals of the derivative spectra should be proportional to the magnetization within experimental accuracy.

It is well established that one may estimate the temperature dependence of the magnetization from the temperature dependence of the intensity of the FMR,[19] such as the data presented in Fig. 5. Previous studies[5,8–10,12] on powder samples have shown that the temperature dependence of the magnetization in $V[TCNE]_x$ can be well approximated by the Bloch form[20]

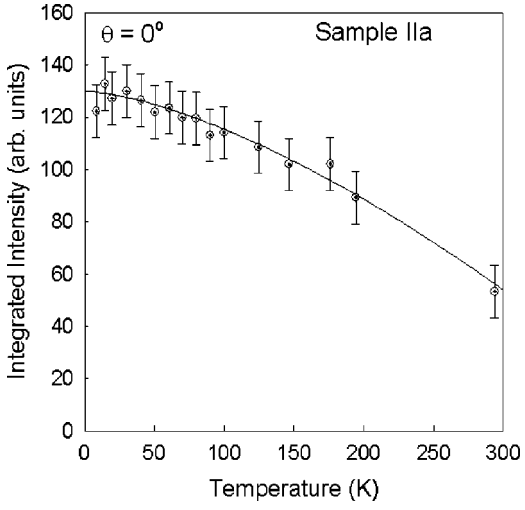

FIG. 5. Integrated intensity of the FMR for $V[TCNE]_x$ for sample IIa. The solid line is a fit to the data as described in the text.

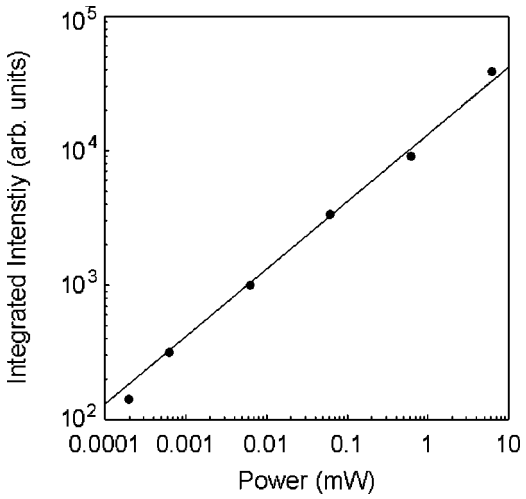

FIG. 6. Dependence of integrated FMR intensity on microwave power. The solid line is a fit assuming the intensity depends on the square root of the power (unsaturated). See text for details.

$$M_s(T) = M_s(0)(1 - BT^{3/2}), \tag{6}$$

where $M_s(0)$ is the magnetization at zero temperature and the parameter B, which characterizes the temperature dependence, is a measure of the ease with which spin waves can be excited.[21] For the fit in Fig. 5, $B=1.13\times10^{-4}$ $K^{3/2}$, and $M_s(0)$ is an arbitrary parameter. [The fits to the temperature dependence of the FMR line positions discussed below yield $M_s(0)=22$ G.] Following the procedure of Ref. 20 one can crudely estimate the critical temperature for this film from the extrapolation to zero. This extimate is $T_c=430$ K, which is in substantial agreement with results presented earlier.[20] For the film used in this study this value of $M_s(0)$ corresponds to 22 emu/g (assuming a density of unity for $V[TCNE]_x$). The values of these parameters are very close to those determined on a similar film using SQUID magnetometry $M_s(0)=14.2$ emu/g, $B=1.13\times10^{-4}$ $K^{3/2}$, $T_c=410$ K).[19,12] Although the SQUID measurements were made at higher fields, at least the low temperature magnetization should not depend strongly on the field.

In Fig. 7 we show the temperature dependence of the magnetic field for a particular FMR spectral feature (zero-crossing for the highest (lowest)-field derivative peak for $\theta=0°$ (90°)] for sample IIb at 300 K. These two features correspond to the same FMR line as will be discussed below. At $\theta=54.7°$ all lines collapse to the same field. Therefore, the data that are shown for $\theta=0°$, 54.7°, and 90° in Fig. 7 correspond to the same individual FMR line. Filled and open symbols in Fig. 7 refer to samples IIa and IIb, respectively. Similar curves were found for the other pairs of spectral features and for all samples studied. The open diamonds in Fig. 7 show data for a CVD-prepared powder sample of $V[TCNE]_x$. Although the values are slightly different than the data at $\theta=54.7°$ in the film, the temperature dependence is essentially the same.

IV. DISCUSSION

We first discuss the role of uniaxial anisotropies in determining the temperature dependence of the FMR in

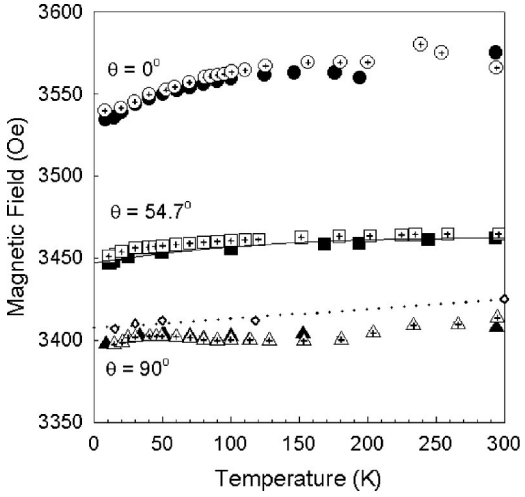

FIG. 7. Temperature dependence of the magnetic field of a particular FMR line for $V[TCNE]_x$ at $\theta=0°$, 54.7°, and 90°. Data for sample IIa and sample IIb are indicated by filled and open symbols, respectively. The open diamonds are data for a CVD-prepared powder sample. See text for details.

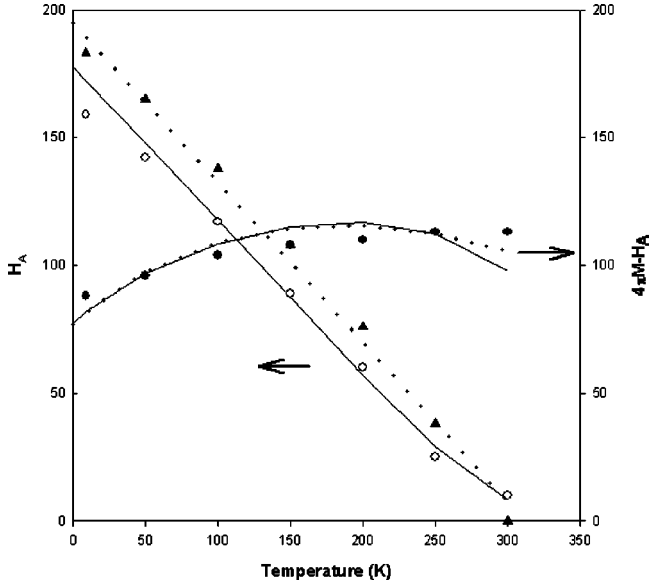

FIG. 8. Extraction of the temperature dependence of the anisotropy field H_A from the positions of the FMR resonances at $\theta=0°$, 54.7°, and 90° for sample IIa (solid triangles and open circles). The solid triangles and open circles are data obtained by assuming that H_A at 300 K is 0 and 10 Oe, respectively. The dotted and solid lines are fits, as described in the text, to the solid triangles and open circles, respectively. The solid circles are $4\pi M-H_A$ as extracted from the data of Fig. 7 as described in the text. The dotted and solid lines are the fits using the dotted- and solid-line fits to H_A shown in the figure. See text for details.

$V[TCNE]_x$. One often adopts the phenomenological approach,[21] which sets $H_A=2K/M$, where K is an anisotropy constant. This phenomenological approach does not work for the present case because it is unable to account for the temperature dependence of the FMR spectra given the observed temperature dependence of M. We therefore adopt a more microscopic approach that was originally developed by Becker for spin glasses[14] in the limit of small remanent magnetization. The philosophy here is that the disorder in the organic, molecular magnets[5–8,13] may be similar to that which exists in spin glasses. In addition, since the remanent magnetization is small for both systems,[13,14] the major approximations made are appropriate for FMR in $V[TCNE]_x$.

We can extract the temperature dependence of H_A from the data of Fig. 7 because we can estimate the temperature dependence of M from the FMR intensity as a function of temperature (Fig. 5). We assume, as will be justified later, that $H_A \simeq 0$ at 300 K. This assumption establishes the absolute value of M at 300 K of 8 G, and the data of Fig. 5 or Eq. (6) determine the values of M at all measured temperatures. In particular, $M(0)=22$ G. We can now determine $H_A(T)$ from the difference between $H(0°)$ and $H(54.7°)$, which is $4\pi M-H_A$. In principle, we could also use the difference between $H(90°)$ and $H(54.7°)$ or between $H(0°)$ and $H(90°)$, but these differences are less accurate, especially at low temperatures. Any inconsistencies will, of course, be reflected in the final fits. The resulting values of H_A are shown as solid triangles in Fig. 8. [The fact that the anisotropy field is negative is taken into account by the sign in Eqs. (2)–(4). These values can then be used with $M(T)$ from Fig. 5 or Eq. (6) to fit the temperature dependence of H_r at any value of θ with no adjustable parameters, but so far the procedure is entirely empirical and relies on the assumption that H_A is negligible at 300 K. The solid and dotted lines in Fig. 8 are fits to the data using the model of Becker,[14] which we now describe.

We first concentrate on the data at low temperatures where the mathematical expressions are simpler. At low temperatures the anisotropy field H_A is directly proportional to the anisotropy constant K and is given by[14]

$$H_A \simeq \frac{K}{\gamma \chi_\perp \omega_0}, \tag{7}$$

where $\chi_\perp$ is the static transverse susceptibility, ω_0 is the angular frequency of the spectrometer, and γ is the gyromagnetic ratio connecting the angular frequency to the internal magnetic field H_0 when M and H_A are zero. The value of γ, which is determined by the spin-orbit coupling, is often expressed as a g-value given by

$$\gamma = \frac{g\mu_\beta}{\hbar}. \tag{8}$$

Experimentally, the temperature dependence of K is often given by[14,22]

$$K(T) = K(0)\left[1 - \frac{2}{3}\frac{T}{T_f}\right], \tag{9}$$

where T_f is a temperature below which the spin system can be considered as frozen in place. The precise meaning of T_f is difficult to define since there exists a wide range of time constants in $V[TCNE]_x$ just as there does in the spin glasses. We therefore take T_f as an adjustable parameter to fit to experiment. We note that although Eq. (7) is only valid at low temperatures, the empirical relationship expressed in Eq. (9) is valid up to $T=3/2\,T_f$, above which $K(T)=0$.

From the values of H_A given as solid triangles in Fig. 8 and Eqs. (7) and (9), the best fit is obtained with $H_A(0) = 195$ Oe and $T_f = 208$ K. This fit is shown by the dotted line in Fig. 8. If one assumes as a rough estimate that $\chi_\perp$ at $T = 0$ is approximately M/H,[13] then using $\chi_\perp = 6 \times 10^{-3}$ one obtains $K(0) = 2 \times 10^2$ erg/cm^3. This value is about a factor of 5 smaller than is typical for ferromagnetic materials where most values fall in the range $10^3 - 10^6$ erg/cm^3.[23]

Since Eq. (9) applies over the complete range of temperatures measured (up to 300 K), we can define an effective (negative) anisotropy field H_A^* for this entire temperature range as follows:

$$H_A^*(T) = \frac{K(T)}{\chi_\perp \omega_0 \gamma}. \tag{10}$$

The complete temperature dependence of H_A, for which Eq. (7) is the low temperature approximation, can now be expressed as[14]

$$H_A(T) = H_0(T) - H_r(T) = \frac{H_A^*(T)}{1 + \alpha \left[\frac{1}{H_A^*(T)} \right]^2}, \tag{11}$$

where

$$\alpha = \frac{M_2^2}{\omega_0^4 \gamma^2 \chi_\perp^2 (kT)^2}, \tag{12}$$

and where following Becker[14] we assume that α is essentially independent of T. (The parameter M_2 represents the relaxation of the time derivative of the magnetization operator, which is assumed to be roughly proportional to T.[14]) For our purposes we consider α as a temperature independent, adjustable parameter. The dotted line fit to H_A shown in Fig. 8 is drawn for $\alpha = 0$, but the near-linear variation of the data (solid triangles) places an upper bound on α of approximately 10, from which one could, in principle, estimate M_2. However, as we shall see the temperature dependence of the FMR linewidth places a much more severe restriction on this parameter.

A more general approach to fitting the data of Fig. 7 to the model of Becker is to consider the magnitude of the magnetization to be variable and use four adjustable parameters [$M(0)$, $H_A(0)$, T_f, and α] to produce the best fit. Such a procedure appears at first glance to produce very ambiguous results, but in fact there is very little flexibility in varying any of these parameters. The reason is that $H_A(T)$ cannot change sign nor can it increase with increasing temperature. These two constraints allow only very limited changes in any of the parameters. In particular, H_A at 300 K must be less than about 15 G. The open circles in Fig. 8 correspond to $H_A(300) = 10$ G, and the solid line is a fit to the data [$H_A(0) = 200$ Oe, $T_f = 246$ K, $M(0) = 255$ G, and $\alpha < 5000$]. This fit does not depend very strongly on α, but the linewidth calculations to be discussed below place a much more stringent limitation ($\alpha < 15$).

Given the agreement between the data and the model fits as shown in Figs. 7 and 9, we have established that the temperature dependence of the FMR line positions is determined by the magnetization and a negative uniaxial anisotropy field. The maximum value of this field is approximately 200 Oe at zero temperature. Previous studies[5–9,13] of the properties of V[TCNE]$_x$ on powder samples prepared in solutions of C_4H_8O (Refs. 5 and 6) and CH_3CN (Refs. 7 and 8) showed greater structural and magnetic disorder, and the analyses yielded much larger anisotropy fields (on the order of 10^4 Oe). Analyses of the magnetic properties of CVD-prepared powder samples[10,12] also led to $H_A \sim 10^4$ Oe in contrast to the value estimated here from FMR studies of CVD-prepared films of V[TCNE]$_x$. Possible origins of the differences in H_A values may be aging, partial oxidation, differences in chemical composition or local structural order, or different assumptions in fitting to the model of Becker.

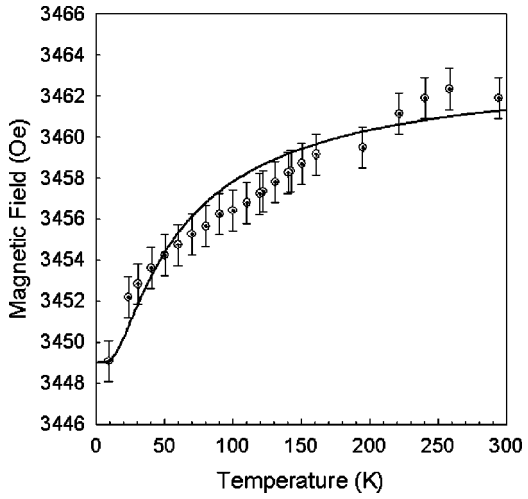

FIG. 9. Temperature dependence of the FMR field at $\theta = 54.7°$ on an expanded vertical scale. The data are for sample IIa. The solid line is a fit to the data as described in the text.

The small value of H_A is not entirely unexpected and may in fact be a general property of structurally ordered organic ferromagnets and ferrimagnets. Recent results for the charge transfer compound tetrakisdimethylamino-ethylene-C_{60} (TRADE-C_{60}) found a very small value of H_A(29 Oe),[24] which is a factor of approximately 10 smaller than the present value obtained for V[TCNE]$_x$. In fact, the models developed for spin glasses are applicable to the semiconducting, amorphous, organic molecular magnets because of the disorder, but there is no *a priori* reason to expect that the parameters will be similar to the amorphous metals.

The fits to the data in Figs. 7 and 8 assume a zero temperature g-value of approximately 1.97, which agrees reasonably well with that observed for CVD-prepared powder samples with no solvent. This fitting procedure precludes the calculation of any changes in the g-value with temperature, which for ferrimagnets should be fairly small.[25,26] However, one may estimate these changes from the spectrum at $\theta = 54.7°$, which is shown on an expanded scale in Fig. 9.

If one ignores the correction term in Eq. (5), then the temperature dependence of the FMR line at 54.7° determines the temperature dependence of $g_{\text{eff}} = h\nu_0/\mu_B H_r$. The correction term in Eq. (5) reaches a maximum value of approximately 0.1% at $T = 0$, and therefore is insignificant compared to the temperature dependence of g_{eff} shown in Fig. 9. The

value of g_{eff} at $T=0$ is consistent with the well-known value of V^{2+} in an octahedral environment, which is approximately 1.98–1.99.[27] At $T=0$ g_{eff} is approximately 1.97. For V^{2+} larger departures from the free electron g-value are usually due to the influence of the covalently bonded ligands.[27] This situation certainly holds for the $V[TCNE]_x$ because the net spin involves unpaired electrons at both the V and TCNE sites.

The detailed mechanism for the temperature dependence of g_{eff} is not known, From earlier magnetic studies of $V[TCNE]_x$ the exchange interaction between $V^{++}(S=3/2)$ and $[TCNE]^{-}(S=1/2)$ is expected to be nearly temperature independent. However, studies of the temperature dependent electrical conductivity of solution prepared powders[28] and temperature and magnetic field dependent conductivity and magnetoresistance of CVD-prepared films[28–30] show an activated electrical conductivity associated with motion of electrons among the $[TCNE]^{-}$. One may therefore propose an admixture of low-lying excited states in these molecular films that is due to thermal averaging.[31] Using the standard spin-orbit correction to the g-value as given by second order perturbation theory and taking the matrix element that admixes the excited state (or states) to be thermally activated, one may write

$$g_{\text{eff}}(T) = g_0 - \Delta g e^{-\Delta E/kT}, \tag{13}$$

where g_0 is the g-value at $T=0$, $g_0-\Delta g$ is the high temperature g-value, and ΔE is the energy difference between the ground and first excited states. Equation (13) is essentially the same as that used successfully for several organic free radicals.[32,33] The solid curve in Fig. 9 is a fit to the data with $g_0=1.967\pm0.001$, $\Delta g=8\times10^{-3}\pm4\times10^{-3}$, and $\Delta E/k=50\pm30$ K. Further theoretical and experimental studies will be necessary to test whether these values are reasonable.

The values of $H_A(T)$ determined from the temperature dependence of the positions of the FMR lines should also affect the linewidths.[14] The linewidths are given by[14]

$$\Delta H(T) = \left[\frac{\alpha}{\mathrm{H}_0\chi_\perp}\right]^{1/2}\frac{H_A(T)}{H_A^*(T)}. \tag{14}$$

Assuming that the linewidth at the lowest temperature (9 K) is entirely determined by Eq. (14), the fit of this equation to the data is shown as the dashed line in Fig. 4 where $\alpha=15$. Even if the high temperature linewidth is determined by anisotropy fields, this mechanism cannot explain the linewidths at lower temperatures. In fact, using reasonable estimates of $\chi_\perp$ in Eq. (14) suggests that even at high temperature this mechanism cannot explain the widths.

The temperature dependences of the individual FMR linewidths in the CVD films are similar to the behavior observed previously in solution prepared powder samples except that the values are always narrower by at least an order of magnitude at any temperature.[13] Long *et al.*[13] fit the temperature dependence of the FMR linewidth in $V[TCNE]_x\ y$(MeCN) to the same model for anisotropic spin glasses as used in the present work and found a consistent fit to the temperature dependences of both the resonant field and the linewidth at temperatures below T_c. The parameters extracted were, in general, very different from those found in the present work. As we have seen, this approach does not work for the CVD-prepared films of $V[TCNE]_x$. Again, the differences may be due to aging, partial oxidation, differences in chemical composition or local structural order, or different assumptions in fitting to the model of Becker.[7,8,13]

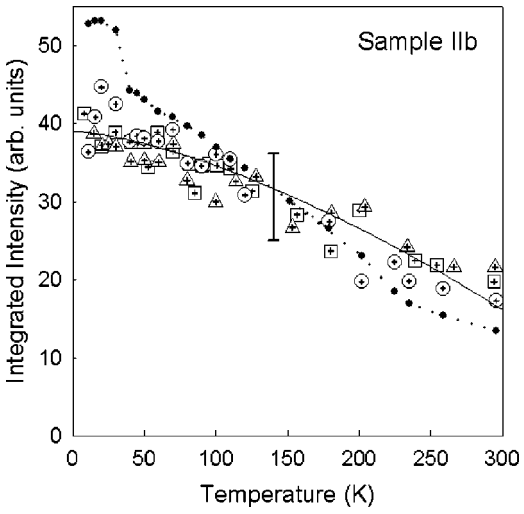

FIG. 10. Comparison of the temperature dependence of the magnetization $M(T)$ (open symbols run at different orientations and different times) and the FMR linewidth ΔH (solid circles) for sample IIb. The solid line is a fit to $M(T)$ as described in the text. The dotted line is an aid to the eye.

In addition to the linewidths being much larger in the powder samples of $V[TCNE]_x\ y$(MeCN), the shift of the resonance frequency from low to high temperature is also much greater. Since the analysis presented above should also apply to these samples, the larger shift implies that the anisotropy field at low temperatures may be about an order of magnitude larger than in the CVD-prepared films. This increase may be due to greater inhomogeneities in the bulk or to the interactions between individual flakes in the powder (in analogy to increases that occur in polycrystalline ferrimagnets[21]).

If H_A is not responsible for the temperature dependence of the linewidths, then one must establish another mechanism. One well established mechanism in polycrystalline and powder samples is porosity or fluctuations in local density, which produce random demagnetization fields.[25,34–37] These fluctuations are due to two-magnon scattering processes.[25] The expression for ΔH is[25,35,36]

$$\Delta H(T) = \frac{16\pi^2}{9}M(T)\frac{(3\cos^2\theta_0 - 1)^2}{\cos\theta_0}P, \tag{15}$$

where P is the porosity, which in the simplest case is given by the sum of the volumes of the pores normalized to the total volume. In Eq. (15), θ_0 depends on the magnetization and the sample geometry. First note that $\Delta H(T)$ depends only on $M(T)$. In Fig. 10 we show the experimentally determined values for these two quantities normalized at low temperature. It is clear that the dependences on temperature are essentially the same. In addition, for a thin film geometry θ_0 is

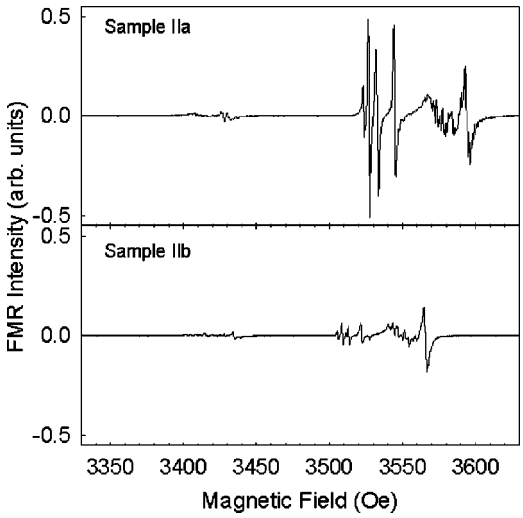

FIG. 11. Comparison of the FMR spectra for $\theta=0°$ for samples IIa and IIb. These samples were deposited in the same run. See text for details.

effectively zero,[25] so a numerical estimate of P can be determined from the data in Fig. 10 and Eq. (15). Given $M=9$ Oe and $\Delta H=3.5$ Oe at 300 K, one obtains $P=6\times10^{-3}$. As the films of $V[TCNE]_x$ are disordered a porosity of $\sim0.5\%$ is reasonable. In addition, many other experiments indicate that the films of $V[TCNE]_x$ are inhomogeneous.[5,28,38]

A second possibility to explain the linewidths is scattering due to surface roughness, which is sometimes called etch pit scattering because it was first observed in etched, single-crystal samples.[25] This mechanism has the same functional form as Eq. (15), where P is replaced by a quantity that depends on the ratio of the radius of the etch pits to the film thickness. Atomic force microscopy measurements on samples similar to those used for FMR show that surface roughness occurs on a scale of about $1-10\%$ of the sample thickness. However, since these experiments were performed in air and it is known that these films are very reactive with oxygen,[2] one cannot rely of the AFM measurements to predict the roughness in the films sealed under an inert atmosphere. Measurements on thinner samples (approximately 0.5 μm thick) exhibit linewidths identical to those observed for the thicker samples. Therefore, we conclude that the FMR linewidths in these films of $V[TCNE]_x$ are probably due to local inhomogeneities that produce density fluctuations rather than dominated by surface roughness.

We now discuss the presence in the FMR spectra of a plethora of narrow lines at 300 K (Fig. 1). These narrow lines for $\theta=0°$ and 90° collapse to a single, narrow line for $\theta=54.7°$ with respect to the normal to the surface of the film. When samples are made in different deposition runs the positions of the lines can be very different as shown in Fig. 1. However, when two macroscopic samples are cut from the same deposition run, the forest of lines is essentially identical as shown in Fig. 11. The reason that the positions of the lines are not exactly the same for samples IIa and IIb is that sample IIb had degraded slightly because it remained many months in the sample tube before the FMR was recorded. (However, this film was still magnetic with a value of T_c above 300 K.) The FMR studies showed that all films studied degraded eventually, presumably due to annealing or oxidation. After degradation the FMR no longer depends on angle; the resonant field approaches that observed in the unoxidized films at 54.7°; and the linewidth at 300 K is approximately 11 Oe, the same as the powder sample shown in Fig. 4.

There are at least four possibilities for the appearance of many sharp lines at 300 K, but only one appears to be plausible in the present case. First, there could be a hyperfine interaction associated primarily with the vanadium atoms. In most vanadium compounds this hyperfine structure consists of eight lines spaced approximately 80 Oe apart. Although there are several reasons why this explanation is unlikely, including the spacings between the lines and the fact that the structure disappears at 54.7°, the most telling is the fact that in ferrimagnetic materials the hyperfine structure is averaged by long-rang exchange coupling.[39]

A second possibility is that the films consist of layers of ferromagnetic material, which are isolated from one another, where each layer possesses a slightly different magnetization. Again, there are several difficulties with this possibility. For example, in some of the films the number of lines exceeds 60. If all of these are due to individual, isolated layers, then for a 1 μm thick film the average layer thickness must not exceed about 10 nm, which should strongly affect the magnetic properties. Also, the individual lines are very narrow indicating that each layer would have to be very well defined, and the narrowest lines appear very regularly in magnetic field, which is unlikely to occur naturally for a series of isolated layers. The most telling difficulty is that the nearly identical spectra in samples IIa and IIb require that any layered structures be homogeneous over macroscopic dimensions, since these two samples were cut from the same film. [In sample IIa (or IIb) there appear to be two or three groups of lines that behave differently as the temperature is lowered. It is possible that these groups of lines each represent a different layer.]

A third possibility is that the features may result from interactions among closely spaced layers such as occur in ferromagnetic multilayer films. This possibility can be rejected for the same reasons discussed in the preceding paragraph.

A fourth possibility is that the sharp features may be due to the presence of spin waves with wave vector $k>0$. The existence of spin waves is by far the most plausible explanation for the structure, but there are also difficulties with this interpretation. For example, the simplest explanation is the existence of spin waves in the linear regime. In this case, when M is always parallel to H, one can show[17] that H in Eq. (1) can be replaced by

$$H^* = H + \frac{2Ak^2}{M}, \tag{16}$$

where A is the exchange stiffness constant and $k=n\pi/d$ $(n=1,3,5,\cdots)$ is the wave number of the spin wave mode. Together Eqs. (1) and (16) predict a series of lines scaling as

n^2, where n is an odd integer. No such spacing is apparent over any extended region in Figs. 1 and 11. In addition, in the simplest case one would expect the spin wave modes to disappear for $\theta=90°$, which is not the case.

Spectra, which are mirror images, such as that shown in Fig. 8, have been seen in thin films of yttrium iron garnet (YIG),[40] where the individual lines are also very narrow (<1 Oe). The appearance of this symmetry is attributed to the presence of second order Suhl instabilities,[41,42] which are nonlinear phenomena involving four magnon scattering.[25] In principle, first order Suhl instabilities, or two-magnon scattering, could be important, but because of the thin film geometry this effect has a large critical microwave field for onset ($h_{\mathrm{crit}} \propto 1/\sin\theta_0$).[25] It is interesting to note that second order Suhl instabilities lead to asymmetries in the derivative lineshapes of the FMR,[39] which are similar to that which we observe for $V[TCNE]_x$ at the lowest microwave fields. This result suggests that the critical microwave field for onset of second order Suhl instabilities in $V[TCNE]_x$ is very low.

The critical field h_{crit} for second order Suhl instabilities can be expressed as

$$h_{\mathrm{crit}} = \frac{\Delta H}{2}\sqrt{\frac{\Delta H_k}{4\pi M}}, \tag{17}$$

where $\Delta H_k = 1/\gamma\tau_k = H_0/\omega_0\tau_\kappa$ and τ_k is the lifetime for a magnon of wave number k. A reasonable lower bound for τ_k is $\Delta\omega^{-1}$ where $\Delta\omega$ is $\gamma\Delta H$. For ΔH approximately 3.5 Oe at 300 K, one obtains $\tau_k > 10^{-7}$ s. (Because ΔH at 300 K is probably dominated by porosity, 10^{-7} s is a lower bound for the relaxation times of the spin waves.) This value of τ_k leads to $h_{\mathrm{crit}} \geqslant 4\times10^{-2}$ Oe. For the spectrometer used in this study, this value corresponds to a critical microwave power that is approximately 0.4 μW, lower than our lowest operating power. Of course, this argument does not guarantee that second order instabilities occur, only that if they do the threshold field is very small. Since most ferromagnetic and ferrimagnetic materials have threshold fields for instabilities that are well below our maximum microwave field (approximately 2 Oe), it is probable that we are in the nonlinear magnon scattering regime at all operating microwave powers. The fact that the individual linewidths are dominated by inhomogeneities is consistent with a low threshold for nonlinear processes.[25,40]

We now examine the consequences of an inhomogeneous sample in producing nonlinear effects,[43] where the equations of motion must include terms higher than those linear in M. (Usually nonlinearities are produced in a uniform sample by an inhomogeneous microwave field, but in this case it is the inhomogeneous sample interacting with a homogeneous microwave field that produces these effects.) Although one cannot fit the forest of lines in the spectra shown in Figs. 1, 3, and 11, the basic features can be understood assuming groups of nonlinear spin waves.

Walker[44,45] has shown that, in the presence of nonlinearities, a series of FMR lines can be observed including sequences where the $k=0$, or Kittel mode, is absent. Unlike the linear spin-wave case discussed above, these series of modes can appear with roughly equal spacings.[44] In addition, unlike the linear case, the spacings between modes scale as the magnetization, and the only effect of H_A is to modify the dc field.[44,45] Finally, from the spacing between the modes, one may obtain an estimate of the exchange interaction constant (exchange stiffness constant) A.

The spacings between the modes generally increase as the temperature decreases roughly proportional to the increase in $M(T)$ with decreasing temperature [Fig. 3(a) and data for samples I and IIb, not shown]. In particular, the spacings increase by approximately a factor of 1.6 between 300 K and 100 K, while $M(T)$ changes by a factor of about 2 over this range. This behavior is consistent with that described above.

One may estimate the magnitude of A in two ways. First, A is given by[43]

$$A = \frac{kT_c a^2 M}{2\gamma h}, \tag{18}$$

where k is the Boltzmann constant, T_c is the critical temperature, a is a lattice constant, and h is Planck's constant. Second, one may express A as[43]

$$A = \frac{(\delta H) M d^2}{4\pi}, \tag{19}$$

where δH is the separation in field between the nearest pairs of lines, and d is the layer thickness. Expression (18) is very similar to that obtained for the smallest separation in the linear case.[36] Using $a \simeq 0.3$ nm and $d \simeq 1$ μm, evaluations of Eqs. (18) and (19) yield the essentially same result, $A \simeq 10^{-10}$ erg/cm. This value is several orders of magnitude smaller than that commonly observed in ferrimagnetic materials such as $Gd_2Fe_{14}B$, where $A \simeq 10^{-6}$ erg/cm.[46] The smaller value for $V[TCNE]_x$ may simply represent smaller exchange between $V^{++}(S=3/2)$ and $[TCNE]^-(S=1/2)$ and the effects of frustration in magnetic ordering[5–7,29] due to antiferromagnetic interactions both between V^{++} and $[TCNE]^-$ and between $[TCNE]^-$ and $[TCNE]^-$.

V. SUMMARY

Ferrimagnetic resonance measurements in thin films of $V[TCNE]_x$ grown by chemical vapor deposition exhibit a series of sharp lines at 300 K. The orientational dependence of these lines is consistent with the well-known effects of sample geometry where the magnetization tracks the applied magnetic field. Double integration of the FMR derivative spectra as a function of temperature yield FMR intensities that track with the temperature dependence of the magnetization as measured by SQUID magnetometry. The temperature dependence of the FMR at various orientations yields an estimate of the temperature dependence of the local, negative anisotropy field, which is approximately 200 Oe at zero temperature and decreases linearly with increasing temperature. This behavior is well fit by a model developed for spin glasses.

The widths of the individual FMR lines increase with decreasing temperature and roughly track the temperature dependence of the magnetization. This behavior suggests that the FMR linewidths are probably determined by density fluctuations in the films.

The spacing between the individual FMR lines and its temperature dependence are consistent with the presence of nonlinear spin waves. The critical microwave field for the appearance of these nonlinearities is approximately 10^{-2} Oe. These characteristic separations provide a rough estimate of the exchange stiffness constant $A=10^{-10}$ erg/cm. The small value of A may be due to the relatively large separation between the vanadium ions in these materials.

ACKNOWLEDGMENTS

Research at the University of Utah was supported by the NSF under Grants No. DMR-9704946 and DMR-0307594, and by a Seed Grant from the University of Utah. R.P. acknowledges support from the University Research Opportunities Program at the University of Utah. K.I.P. and A.J.E. at the Ohio State University and J.S.M. at the University of Utah acknowledge support by the Department of Energy under Grant Nos. DE-FG02-01ER45931, FG02-86ER45271, by DARPA through an ONR Grant No. N00014-02-1-0593, and by the Army Research Office. The authors thank C. Inglefield for performing the atomic force microscopy experiments.

[1] J. S. Miller and A. J. Epstein, J. Chem. Soc., Chem. Commun. **1998**, 1319.
[2] J. M. Manriquez, G. T. Yee, R. S. McLean, A. J. Epstein, and J. S. Miller, Science **252**, 1415 (1991).
[3] J. Zhang, P. Shou, W. B. Brinckerhoff, A. J. Epstein, C. Vazquez, R. S. McLean, and J. S. Miller, ACS Symp. Ser. **644**, 1 (1996).
[4] J. S. Miller and A. J. Epstein, MRS Bull. **25**, 21 (2000); A. J. Epstein, *ibid.* **25**, 33 (2000); **28**, 492 (2003).
[5] A. J. Epstein and J. S. Miller, Mol. Cryst. Liq. Cryst. **233**, 171 (1993).
[6] P. Zhou, S. M. Long, J. S. Miller, and A. J. Epstein, Phys. Lett. A **181**, 71 (1993).
[7] P. Zhou, B. G. Morin, J. S. Miller, and A. J. Epstein, Phys. Rev. B **48**, 1325 (1993).
[8] P. Zhou, J. S. Miller, and A. J. Epstein, Phys. Lett. A **189**, 193 (1994).
[9] W. B. Brinckerhoff, J. Zhang, J. S. Miller, and A. J. Epstein, Mol. Cryst. Liq. Cryst. **272**, 417 (1995).
[10] K. I. Pokhodnya, A. J. Epstein, and J. S. Miller, Adv. Mater. (Weinheim, Ger.) **12**, 410 (2000).
[11] D. de Caro, M. Basso-Bert, J. Sakah, H. Casellas, J.-P. Legros, L. Valade, and P. Cassoux, Chem. Mater. **12**, 587 (2000).
[12] K. I. Pokhodnya, D. Pejakovic, A. J. Epstein, and J. S. Miller, Phys. Rev. B **63**, 174408 (2001).
[13] S. M. Long, P. Zhou, J. S. Miller, and A. J. Epstein, Mol. Cryst. Liq. Cryst. **272**, 429 (1995).
[14] K. W. Becker, Phys. Rev. B **26**, 2409 (1982); **26**, 2394 (1982).
[15] Details are available in B. Yan, N. A. Schultz, A. L. Efros, and P. C. Taylor, Phys. Rev. Lett. **84**, 4180 (2000); B. Yan and P. C. Taylor, Mater. Res. Soc. Symp. Proc. **507**, 787 (1998).
[16] M. Ondris and Z. Frait, Czech. J. Phys., Sect. B **11**, 883 (1961); P. E. Tannenwald and M. H. Seavy, Jr., Phys. Rev. **105**, 377 (1957).
[17] P. W. Wigen, C. F. Kooi, M. R. Shanabarger, and T. D. Rossing, Phys. Rev. Lett. **9**, 206 (1962).
[18] M. J. Pechan, M. B. Salamon, and I. K. Schuller, J. Appl. Phys. **57**, 3678 (1985); **59**, 3302(E) (1986).
[19] See, for example, M. Farle, Rep. Prog. Phys. **61**, 755 (1998), and references therein.
[20] F. Bloch, Z. Phys. **61**, 206 (1930).
[21] See, for example, M. G. Cottam and A. N. Slavin, in *Linear and Nonlinear Spin Waves in Magnetic Films and Superlattices*, edited by M. G. Gottam (World Scientific, Singapore, 1994), p. 1.
[22] S. Schultz, E. M. Gullikson, D. R. Fredkin, and M. Tovar, Phys. Rev. Lett. **45**, 1508 (1980).
[23] See, for example, G. V. Skrotskii and L. V. Kurbatov, in *Ferromagnetic Resonance*, edited by S. V. Vonovskii (translated by H. S. H. Massey) (Pergamon, New York, 1966), p. 12.
[24] D. Arcon, P. Cevc, A. Omerzu, and R. Blinc, Phys. Rev. Lett. **80**, 1529 (1998).
[25] C. W. Haas and H. B. Callen, in *Magnetism*, edited by G. T. Rado and H. Suhl (Academic, New York, 1963), Vol. I, p. 449.
[26] R. K. Wangsness, Phys. Rev. **119**, 1496 (1960).
[27] A. Abragam and B. Bleaney, *Electron Paramagnetic Resonance of Transition Metal Ions* (Clarendon, Oxford, 1970), p. 432.
[28] G. Du, J. Joo, A. J. Epstein, and J. S. Miller, J. Appl. Phys. **73**, 6566 (1993).
[29] V. N. Prigodin, N. P. Raju, K. I. Pokhodnya, J. S. Miller, and A. J. Epstein, Adv. Mater. (Weinheim, Ger.) **14**, 1230 (2002).
[30] N. P. Raju, T. Savrin, V. N. Prigodin, K. I. Pokhodnya, J. S. Miller, and A. J. Epstein, J. Appl. Phys. **93**, 6799 (2003).
[31] R. E. Moss and A. J. Perry, Mol. Phys. **22**, 789 (1971).
[32] M. T. Jones, T. C. Kuechler, and S. Metz, J. Magn. Reson. (1969-1992) **10**, 149 (1973).
[33] G. Vincow, M. L. Morrell, F. R. Hunter, and H. J. Dauben, Jr., J. Chem. Phys. **48**, 2876 (1968).
[34] S. E. Harrison, H. S. Belson, and C. J. Kriessman, J. Appl. Phys. **29**, 337 (1958).
[35] M. Sparks, R. Loudon, and C. Kittel, Phys. Rev. **122**, 791 (1961).
[36] E. A. Turov, in *Ferromagnetic Resonance*, edited by S. V. Vonovskii (translated by H. S. H. Massey) (Pergamon, New York, 1966), p. 184.
[37] E. Schlomann, Conference on Magnetism and Magnetic Materials, 1956 (1957).
[38] D. Haskel, Z. Islam, J. Lang, C. Kmety, G. Srajer, K. I. Pokhodnya, A. J. Epstein, and J. S. Miller, Phys. Rev. B (to be published).
[39] See, for example, O. Fedorych, M. Byszewski, Z. Wilamowski, M. Potemski, and J. Sadowski, Acta Phys. Pol. A **102**, 617 (2002).
[40] P. Dorsey, J. B. Sokoloff, and C. Vittoria, J. Appl. Phys. **74**, 1938 (1993).

[41] P. W. Anderson and H. Suhl, Phys. Rev. **100**, 1788 (1955).
[42] H. Suhl, J. Appl. Phys. **29**, 416 (1958).
[43] V. G. Bar'yakhtar and M. I. Kaganov, in *Ferromagnetic Resonance*, edited by S. V. Vonovskii (translated by H. S. H. Massey) (Pergamon, New York, 1966), p. 231.
[44] L. R. Walker, J. Appl. Phys. **29**, 318 (1958).
[45] L. R. Walker, Phys. Rev. **105**, 390 (1957).
[46] S. E. Bushnell, P. C. Dorsey, W. B. Nowak, and C. Vittoria, J. Appl. Phys. **73**, 6491 (1993).